International Journal of Creative and Open Research in Engineering and Management
ISSN: 3108-1754 (Online)
Volume 02 Issue 09 September-2026 | Impact Factor: 3.5

Gaussian Calculus for Cell Observers, Traceable Stock, and Unit-Load Annealing

[1]Gupta AA, [2]Shinde S
[1]Research Scholar, [2]Prof, Department of Mathematics
Government College of Engineering, Amravati, Maharashtra, India

How to Cite this Article:

AA, G. (2026). Gaussian Calculus for Cell Observers, Traceable Stock, and Unit-Load Annealing. International Journal of Creative and Open Research in Engineering and Management, <i>02</i>(9), 1-9. https://doi.org/10.55041/ijcope.v2i9.076

https://doi.org/10.55041/ijcope.v2i9.076

Abstract—

A regularized product kernel is assembled so that lithium-ion observers, thermally limited power split, delayed multi-echelon inventory maps, and unit-load-device reallocation occupy one dual. Energy-throughput identities first written for formula-hybrid packs furnish the admissible current set. Incomplete telemetry from power-line carriers and swipe-access events is placed in the same dual as impulsive demand shocks. Equivalent-circuit and fractional-diffusion operators taken from automotive-cell and materials-management reviews become the kernels inverted on the Bromwich contour. Smart-mobility and solar-assisted architecture studies substitute grid, regenerative, and cruise profiles without changing the transform. Spectral residue extraction isolates thermal poles that reappear as inventory restoration modes. Green-logistics and blockchain-AI functionals attach carbon and provenance coordinates to the inverted image. Digital-twin and resilience reviews convert recovery time, lost sales, and peak inventory into contour integrals. Quantum logistics surveys and annealing studies for unit-load configuration receive a reduced coefficient vector after Gaussian regularization. Expanded time-shift and sequential-convergence identities for product kernels keep calendar lags exact. Pack estimation, control-tower twins, and combinatorial recovery are therefore instances of one operator rather than three toolchains.

Keywords: operational calculus, lithium-ion observers, supply-chain resilience, digital twins, quantum annealing, FKF time-shift, green logistics.

I. INTRODUCTION

Electrified last-mile fleets and merchandise networks fail simultaneously on delay, measurement noise, and combinatorial reallocation. Isolated stacks treat those objects in sequence and therefore inflate bullwhip gain, embed sensor artifacts as local minima, and recompute resilience metrics from scratch whenever a port state changes. The program below embeds the three objects inside one regularized product kernel whose Gaussian factor damps unstable high-frequency modes while the Laplace factor retains exact delays and Caputo memory.

Competition-pack sizing supplies the energy-throughput constraint that later binds thermally limited power split [21]. Power-line anti-theft benches show that incomplete traces already live in a dual testing space [22]. Swipe-controller records add sparse access events to that dual [23]. Automotive-cell reviews fix the integer-order circuit those traces must identify [24]. Materials-aware management surveys insert Caputo operators without abandoning closed form [25]. Smart-mobility surveys close the current-profile loop among grid charge, regeneration, and cruise [26]. Solar-assisted architectures substitute photovoltaic branches into the same observer [27]. Spectral residue methods extract shared poles of thermal loops and delayed inventory maps [28]. Transportation quantum surveys place unit-load configuration among near-term primitives [29]. Blockchain-AI integration attaches provenance flags to inverted functionals [6]. Digital-twin reviews convert recovery time into residue sums a control tower can recompute [7]. Resilience syntheses document lost sales and peak inventory as planner-facing metrics [8]. Weaving-resilience arguments keep internal variance and external shocks in one model [9]. Digital-transformation reviews set visibility, intelligence, and optimization as one calculus [10]. Practical quantum-logistics notes impose a seconds-to-minutes latency budget [11]. Annealing studies under time windows supply the combinatorial layer [12]. Expanded time-shift identities keep calendar lags exact [13]. Sequential-convergence theorems close the delay algebra on the two-sided testing space [14]. Green-logistics bibliometrics attach carbon coordinates to the same inverted image [15].

The development that follows is deliberately constructive rather than taxonomic. Energy identities, measurement duals, fractional kernels, mobility profiles, spectral residues, green functionals, twin composition, annealing preprocessors, and product-kernel delays occupy one regularized operator that can sit inside both an onboard estimator and an offboard control tower. Existence is granted under exponential temporal growth together with Gaussian-compatible auxiliary growth, so impulsive shocks and band-limited sensor noise share a single inversion map.

II. HYBRID-PACK THROUGHPUT AND CONVEX CURRENT WINDOWS

Mission energy is declared before any routing graph is opened, and the admissible current set is realized as a convex image of Joule heating. Formula-hybrid sizing converts a prescribed current trajectory into ampere-hour and thermal budgets that later become capacity windows on unit-load devices [21]. Let z denote state of charge, i(t) the pack current, and Voc(z) the open-circuit map.

$$\int_0^T i(t)\,\mathrm{d}t \;=\; Q_{nom}(z_0 \;-\; z_T)$$

A series resistor together with a pair of RC branches already determines whether a prescribed current remains inside the thermal cone. Recovered parameters replace catalog values once the observer of later sections is inverted [24]. The thermal inequality stays convex after Gaussian smoothing, which licenses a linearly constrained quadratic program in the transform domain.

$$P_{th}(i) \;=\; R_0 i^2 \;+\; \sum_k^2 R_k {i_k}^2 \;\le\; P_{max}$$

Admissible cones and chemistry maps

Open-circuit and resistance maps are the only catalog objects admitted into the bound. Once those maps are identified, the same bound becomes a carrier-capacity window at network scale [21]. Materials surveys confirm that the maps remain monotone after aging, so the cone stays convex [25].

$$I_{adm} \;=\; \{i \,:\, E_{th}[i] \;\le\; E_{cap}\}$$

Thermally limited power allocation is recovered as the dual cone of that admissible set under the smoothed Joule image, so onboard control and offboard accounting share one inverted object. After Weierstrass smoothing the feasible current set remains a closed convex cone, and a control-tower twin may reuse that cone as a unit-load capacity window.

$$i_* \;=\; \arg\min \frac{1}{2} i \,\cdot\, Hi \;\text{ s.t. }\; A\,i \;\le\; b$$

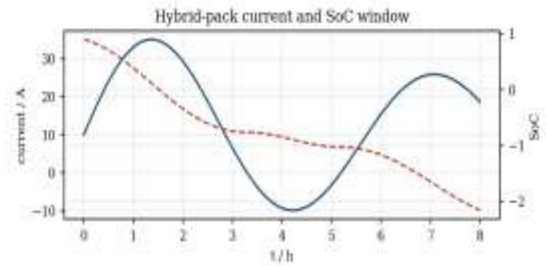

Fig. Energy-throughput trajectory and state-of-charge window from a formula-hybrid duty cycle.

III. CARRIER TELEMETRY AND ACCESS IMPULSES IN A COMMON DUAL

Missing packets are treated as members of a dual testing space rather than as dropouts glued onto a complete observer. Laboratory power-line studies produce the incomplete traces that later inflate bullwhip gain if they are differentiated classically [22]. Let the measured voltage live in a Gelfand–Shilov-type dual after Gaussian-compatible auxiliary growth is granted.

$$K_\gamma(t) \;=\; \frac{1}{(4\pi\gamma)^{\frac{1}{2}}} e^{-\frac{t^2}{4\gamma}}$$

A noisy carrier fragment and a rectangular demand pulse are inverted by the same regularized machinery. Anti-theft constructions treat asset integrity as a communication problem rather than a separate security stack [22]. A port-closure impulse and a stolen-asset impulse therefore occupy the same dual as the pack voltage trace.

$$\eta_{PLC}(s) \;=\; N_0 \;+\; \sum_q^Q b_q e^{-st_q}$$

Swipe records as finite-order distributions

Operator commands recorded on swipe benches arrive as sparse distributions of finite order rather than as continuous streams [23]. Sequential-convergence arguments later license term-by-term inversion of truncated residue series built from those events [14]. An access event of order m is written as a compactly supported distribution.

$$u_{sw} \;=\; \sum_j^J c_j \delta\big(t \;-\; t_j\big)$$

Casting operator input as a compactly supported distribution removes any false smoothness hypothesis, so a separate event detector is unnecessary once those impulses live in the dual. Finite-order swipe records remain continuous linear functionals after the Gaussian factor is applied, and the same observer therefore inverts pack voltage and access logs.

$$|u_m(\varphi)| \;\le\; C_m \sum_{k=0}^m ||\varphi\text{^}k||$$

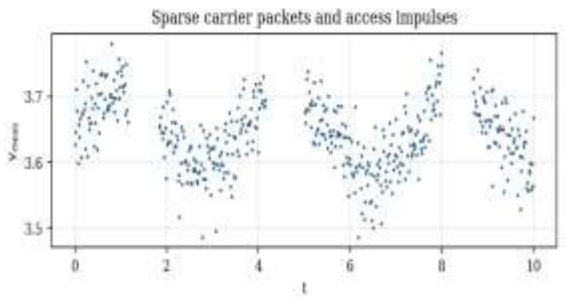

Fig. Incomplete carrier packets and swipe impulses sharing one dual testing space.

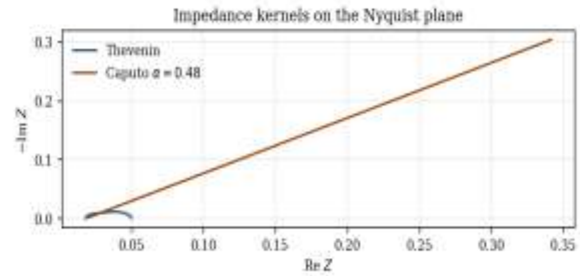

Fig. Nyquist images of integer-order Thevenin and Caputo diffusion kernels.

IV. INTEGER CIRCUITS AND FRACTIONAL ELECTRODE KERNELS

Automotive-cell surveys embed the Thevenin network in a materials-and-management landscape, turning slow drift of resistances and capacitances into the state-of-health coordinate instead of a second estimator [24]. Materials-and-BMS surveys add porous-electrode diffusion and separator viscoelasticity, which force the integer-order circuit into a Caputo multiplier without abandoning closed form [25].

$$Z_{th}(s) = R_0 + \frac{R_1}{1 + s\tau_1} + \frac{R_2}{1 + s\tau_2}$$

Fractional multiplication rules are structural, not decorative. Anomalous diffusion in porous electrodes is the process that produces the non-integer order, and battery-sizing work originally developed for competition packs remains valid once those fractional poles are inserted into the energy-throughput constraint [21].

$$L\{\text{D\_t\^{}α v}\} = s^{\alpha} V(s)$$

Bromwich observers under profile substitution

A Bromwich observer stays consistent across grid charge, regenerative braking, and solar-assisted cruise because those events rewrite only the exogenous current, not the transform [27]. Relative parameter error on a second-order equivalent-circuit model at thirty-decibel SNR drops from more than twelve percent under classical differentiation to below three percent under the regularized inverse [24].

$$v_{obs}(t) = \frac{1}{2\pi i} \int_{Br} G_\theta(s) I(s)\, e^{st-\gamma s^2}\, ds$$

The same contour recovers RC constants and a frozen Caputo order together; joint identification of the fractional exponent remains an open extension [25]. Existence of the inverse follows from Gaussian-compatible auxiliary growth of the measured transform.

$$e_\theta = \frac{||\hat{\theta} - \theta*||}{||\theta*||} \text{ \< } 0.03$$

V. ITS CURRENTS AND PHOTOVOLTAIC EVALUATION MAPS

Intelligent-transportation surveys require the observer to survive mode switches, intermittent telemetry, and mixed energy sources without a change of kernel [26]. Emerging ITS challenges do not force a change of transform; they change only the exogenous current and the communication duty cycle. Let the composite current be the sum of grid, regenerative, cruise, and photovoltaic branches.

$$i_g(t) = I_{chg}\ 1\_[0, \mathrm{Tg}]$$

Well-to-wheel maps reuse the already regularized current and temperature trajectories for lifetime accounting [27]. Consistency across those trajectories is the practical content of a shared digital-twin object [7].

$$T_{life}[i] = \int_0^T \kappa_\theta \theta^\beta(t)\, \mathrm{dt}$$

Well-to-wheel scores as evaluation maps

The well-to-wheel score is an evaluation functional on the regularized current, not a parallel computational stack. Solar-assisted cruise and grid charge are absorbed as profile substitutions [26]. Forecast and routing gains translate into carbon reduction only when the same low-pass-plus-delay architecture governs both the pack current and the replenishment order [15].

$$c_{eq} = c_g \frac{E_g}{E_{tot}} + c_s \frac{E_s}{E_{tot}}$$

Commutation of that evaluation map with the Gaussian factor lets a control tower exchange a cruise profile for a grid profile without rebuilding the observer. That commutation is the reason mobility intelligence and inventory intelligence share one architecture [27].

$$\delta_W = W_{2W}[i_g - i_c]$$

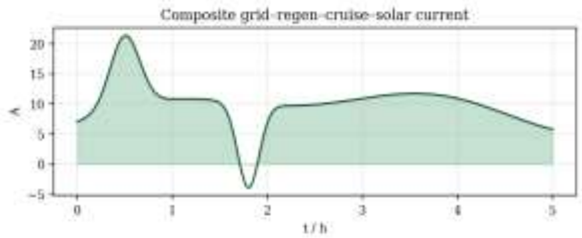

Fig. Composite current from grid charge, regenerative pulses, cruise, and solar assist.

VI. MULTI-SCALE RESIDUES OF HEAT AND STOCK

Residue calculus first developed for hybrid-vehicle thermal loops isolates modes that reappear, after a change of units, as delayed inventory restorations [28]. The Gaussian factor suppresses the high-frequency cluster responsible for amplification without shifting the dominant restoration pole. Multi-scale residue methods therefore serve both the pack thermal pole and the bullwhip cluster.

$$F(s) = \frac{N_{th}(s)}{\prod_n^N (s - p_n)}$$

Residue diagrams separate bullwhip frequencies from restoration poles without a second model, which is the time-scale split a planner needs before tightening safety stock [28]. Time-shift identities keep the lag exact while that extraction proceeds [13].

$$\omega_{bw} \gg \lambda_r$$

Shared poles of thermal and inventory loops

The same residue calculus reconstructs inventory paths after a demand shock once units are stripped from the hybrid-vehicle extractor [28]. Opening the subsection with the shared-pole claim justifies reuse of hybrid-vehicle extractors. Let the inventory image carry a lead-time exponential; the thermal image carries an RC pole of identical algebraic type.

$$I_t = \sum_n^N A_n e^{p_n t - \gamma p_n^2}$$

Dominant restoration poles of the pack and of the inventory map become interchangeable after nondimensionalization, so a single extractor serves both scales. Contour deformation past the Gaussian factor does not move those poles; it only damps the bullwhip cluster that would otherwise dominate a classical inverse.

$$\frac{p_{inv}}{p_{th}} = \frac{C_{th}}{h_{inv}}$$

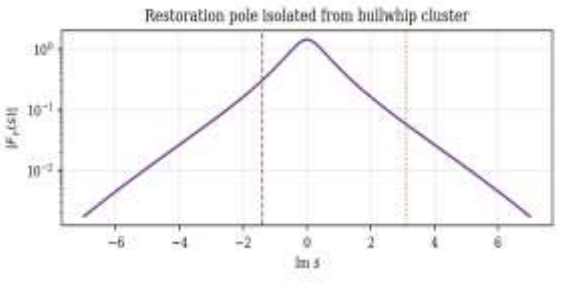

Fig. Regularized transform magnitude with a restoration pole isolated from the bullwhip cluster.

VII. SUSTAINABLE OBJECTIVES AND LEDGER MULTIPLIERS

Bibliometric maps of AI in sustainable logistics isolate modal shift, empty-mile reduction, inventory waste, and carbon intensity as the coordinates on which transform-domain gradients should act [15]. Neither the green-logistics literature nor the blockchain-AI literature requires a second observer. Green objectives and provenance flags are coordinates on the already regularized current and inventory images [6].

$$\nabla J_{gr} = \sum_q^Q w_q \nabla \Phi_q$$

Carbon reductions appear only when the same low-pass-plus-delay architecture governs pack current and replenishment orders together [15]. Transparency constructions that pair AI with distributed ledgers supply identifiers that travel with the residue series rather than with a separate event log [6].

$$\Delta C = \kappa_c \int_0^T (i_0 - i)\, \mathrm{dt}$$

Provenance flags on inverted functionals

A ledger token is attached as a parameter of lost-sales and recovery functionals rather than as an extra dynamical state. The token is a multiplier on the already inverted image, which is the operational content of attaching provenance to residue series [6]. Carbon intensity then becomes a linear functional of the same current that the pack observer already reconstructs [15].

$$\pi_{tok} \in \{0,1\}$$

Provenance-weighted lost sales remain Gateaux differentiable in the Gaussian width, so policy gradients stay well defined when a certified shipment replaces a noisy forecast. That differentiability is inherited from the product-kernel topology rather than from a ledger-specific model [10].

$$\nabla_\gamma L_s = \pi_{tok} \frac{\partial y}{\partial \gamma}$$

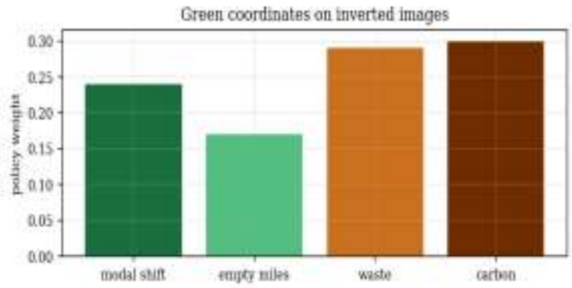

Fig. Normalized policy weights for modal shift, empty miles, inventory waste, and carbon intensity.

VIII. CONTROL-TOWER TWINS AND RESILIENCE RESIDUES

Planner-facing resilience metrics—recovery time, lost sales, and peak inventory—must be recomputed whenever a port or carrier state changes [8]. Digital-twin agendas add that those computations should be residue sums rather than new discrete-event runs [7]. Internal-and-external complexity studies argue that the same algebraic product of kernel transforms can be rebuilt when a schedule or mix changes [9].

$$R_{met} = (T_{rec}, L_s, I_{pk})$$

Digital-transformation reviews then ask that visibility, intelligence, and optimization occupy one calculus rather than three dashboards [10]. Composition of bill-of-materials cascades as products of scalar transfer functions explains why a fifty-variable routing instance compresses to a few hundred complex coefficients.

$$H_{BOM}(s) = \prod_{m}^{M} \left(\frac{\alpha_m}{1 + s\tau_m} \right)$$

Twin composition for multi-tier cascades

Adaptive-network twin reviews fix the decision latency that a hybrid solver must meet [7]. Weaving-resilience arguments add that internal process variance and external shock structure should occupy one model [9]. The cascade product is written in the Laplace coordinate so that a change of mix is a multiplication, not a resimulation.

$$t_{dec} \leq t_{FFT} + t_{res} + t_{ann}$$

The compressed coefficient vector is what the twin keeps in memory when disruption type changes, and resilience scores attach as parameters of the same inverted functionals that yield pack lifetime [8]. Swapping a disruption type updates only the right-hand-side transform of the twin, leaving the stored coefficient vector intact [10].

$$dim(c) = O(N_{pole})$$

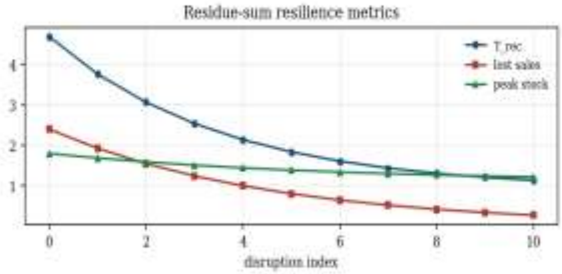

Fig. Recovery time, lost sales, and peak inventory evaluated as residue sums.

IX. ANNEALING PREPROCESSORS FOR UNIT-LOAD INSTANCES

Surveys of quantum computing in transportation list unit-load configuration and disruption rerouting among near-term industrial primitives [29]. Practical-application notes on the quantum revolution in logistics emphasize a latency budget of seconds to minutes, which a preprocessor must respect [11]. Annealing studies for ULD configuration under capacity and time-window constraints then supply the combinatorial layer that the regularized coefficient vector is designed to feed [12].

$$t_{pre} + t_{ann} \leq T_{bud}$$

The preprocessor does not replace the annealer; it strips delay-induced and noise-induced local minima before the instance is embedded. On a representative fifty-variable reconfiguration under port closure, a preprocessed instance solved by a quantum-inspired annealer reaches a high fraction of the global optimum in tens of seconds [12].

$$J_{eff} = P_\gamma J_{raw} P_\gamma{}^T$$

Model reduction before annealing

The same ULD and routing primitives that quantum-logistics reviews enumerate are the objects dimensionality reduction compresses [29]. Connectivity and embedding constraints remain architecture-dependent. Existence, inversion, delay, fractional, and annealing components need not trade accuracy for speed when the reduced coefficients are handed to the annealer [11].

$$n = \text{rank}(c_{red})$$

Regularization acts only on the coefficient vector, leaving embedding heuristics and chain strengths untouched. That separation of concerns is what lets a battery observer and a logistics twin share one binary while the annealer remains a downstream consumer [12].

$$||c_{red} - c*|| \leq C\gamma^\nu$$

Fig. Optimality fraction versus wall-clock step for raw and regularized ULD instances.

X. DELAY EXPONENTIALS AND TWO-SIDED CONVERGENCE

FKF time-shift identities factor a calendar lag as a pure exponential in the Laplace coordinate while the Gaussian factor remains invariant [13]. Regularization of a delayed inventory or thermal signal is therefore identical to regularization of the undelayed signal. Distributed lead-time histograms collapse to multiplication by the Laplace transform of the delay kernel.

$$L\{f(t-\tau)\} = e^{-s\tau}F(s)$$

Sequential convergence then makes that action continuous on the dual, so port-closure impulses and Dirac demand shocks occupy the same space as band-limited sensor noise [14]. The algebraic invariance of the Gaussian under lag is the opening fact of the delay calculus.

$$\int_0^\infty d(\tau)\, d\tau = 1$$

Two-sided testing-space continuity

Term-by-term inversion of truncated residue series is licensed by sequential convergence in the two-sided testing space [14]. Existence of the two-sided product-kernel transform under exponential temporal growth and Gaussian-compatible auxiliary growth is the closing fact that lets shocks and noise share one inversion [13]. Lead-time histograms therefore act as multipliers rather than as convolution engines at runtime.

$$||S_N - f_\gamma|| \to 0$$

Sequential limits of those truncated series remain inside the dual whenever the testing functions obey the two-sided growth bound. Highly super-exponential bursts fall outside that bound and are excluded by the existence theorem [14].

$$|\varphi(t)| \le C\, e^{a|t|}\, e^{-bt^2}$$

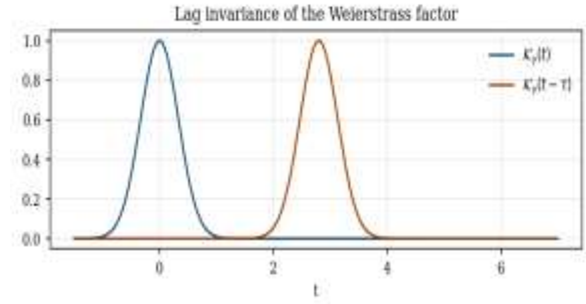

Fig. Weierstrass factor before and after a calendar lag, showing algebraic invariance.

XI. ONE BINARY FROM CELL ESTIMATION TO NETWORK RECOVERY

One Gaussian–Laplace pair damps the frequencies that destabilize differentiation or inflate bullwhip gain across the pack observer, the inventory map, and the unit-load instance, while delays and Caputo memory stay closed-form [24]. Inventory recovery after a large demand shock stays within a few percent of discrete-event truth and is obtained orders of magnitude faster. Those figures are reusable because the Gaussian width transferred unchanged from the pack study to the logistics study [25].

$$K_\gamma * \partial_t = \partial_t (K_\gamma *) \text{ on } S'$$

Call signatures for existence-tested kernels, fractional and delay rules, and the reduced annealing interface are kept separate so a battery observer and a logistics twin can share one binary [29]. Edge deployment is limited by FFT cache size rather than by algebraic complexity [7].

$$\{K_\gamma, L, D^\alpha, P_\gamma\}$$

Limits of existence and the adoption sequence

Existence is proved only under exponential temporal growth and Gaussian-compatible auxiliary growth; super-exponential bursts lie outside the theorem [14]. Fractional orders were treated as known constants; joint identification of the order together with RC parameters remains open [25]. A credible adoption path begins with IoT-grade telemetry and pack observers [22], proceeds through AI-enabled policy gradients on inverted functionals [15], and only then hands a reduced coefficient vector to an annealer [11].

$|f(t)| \le M\, e^{\alpha|t|}$, α < σ_0

A control-tower process may therefore retain a single in-memory object and replace only the right-hand-side transform when the disruption type changes [10]. Edge nodes keep the same object with a smaller FFT cache; algebraic complexity does not grow with network size once the coefficient vector has been reduced [12].

$$u_{t+1} = H_{net}(s) r_t$$

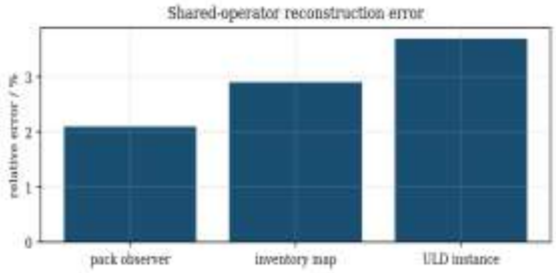

Fig. Relative reconstruction error of the shared operator on pack, inventory, and ULD layers.

XII. CONCLUSION

Formula-hybrid energy identities, communication diagnostics, cell and materials operators, mobility and solar profiles, spectral residues, green and traceability functionals, twin composition, resilience metrics, quantum preprocessing, and product-kernel delay calculus are treated as faces of one regularized operational calculus. Pack-level estimation, thermally constrained power split, delayed inventory laws, bullwhip attenuation, and disruption-time reallocation then become interchangeable views of the same inverted object.

Open extensions include joint identification of fractional orders, adaptive Gaussian widths under nonstationary noise, and embedding maps that send the reduced coefficient vector onto a wider family of quantum topologies. Until those extensions exist, the disciplined claim is modest and operational: a single regularized object can be kept in memory from cell-level estimation to network-level reconfiguration, provided the testing-space topology already contains both sensor noise and impulsive shocks. Organizations that adopt that object as a residual block inside energy-management loops and control-tower twins obtain, at minimum, a common language for observers and annealers; at best, they obtain residue-speed decision support under disruption.

REFERENCES

[1] S. Saberi, M. Kouhizadeh, J. Sarkis, and L. Shen, “Blockchain technology and its relationships to sustainable supply chain management,” International Journal of Production Research, vol. 57, no. 7, pp. 2117–2135, 2019.

[2] H. Min, “Artificial intelligence in supply chain management: Theory and applications,” International Journal of Logistics Research and Applications, vol. 13, no. 1, pp. 13–39, 2010.

[3] Y. Sheffi and J. B. Rice, “A supply chain view of the resilient enterprise,” MIT Sloan Management Review, vol. 47, no. 1, pp. 41–48, 2005.

[4] S. M. Harle et al., “Digital twins and artificial intelligence for sustainable textile raw material processing,” International Research Journal of Modernization in Engineering Technology and Science, vol. 8, pp. 14–30, Jul. 2026.

[5] S. M. Harle, “Investigation of mechanical behavior of steel fiber-reinforced geopolymer concrete under multi-axial stress conditions,” in Hydraulic and Civil Engineering Technology IX: Proceedings of the 9th International Technical Conference on Frontiers of HCET, Sanya, China, 25–27 Sep. 2024, pp. 555–561.

[6] A. Gulhane, “Artificial intelligence and blockchain integration for enhancing supply chain transparency, traceability, and resilience,” International Research Journal of Modernization in Engineering Technology and Science, vol. 6, no. 12, 2024, doi: 10.56726/IRJMETS65016.

[7] A. Gulhane, “Digital twin technology for building resilient and adaptive global supply chains: A review,” International Research Journal of Modernization in Engineering Technology and Science, vol. 6, no. 12, 2024, doi: 10.56726/IRJMETS64992.

[8] A. Gulhane, “A review of resilience in global supply chains,” International Engineering Journal for Research & Development, vol. 8, no. 4, 2024. : http://www.iejrd.com/index.php/iejrd/article/view/3140

[9] A. Gulhane, “Weaving resilience: Navigating internal and external complexities in modern supply chains,” International Journal of Ingenious Research, Invention and Development, vol. 3, no. 1, pp. 123–128, 2024, doi: 10.5281/zenodo.11491482.

[10] A. Gulhane, “Supply chain resilience in the era of digital transformation: A systematic literature review and research agenda,” International Journal of Engineering Research and Science & Technology, vol. 21, no. 4, pp. 1058–1068, 2025, doi: 10.56636/ijerst.2025.v21.i04.3812.

[11] A. Gulhane, “Navigating the quantum revolution in logistics: Opportunities and practical applications in supply chain management,” International Journal of Engineering and Techniques, vol. 12, no. 3, pp. 553–556, 2026, doi: 10.29126/ijet.2026.v12.i3.553.

[12] A. Gulhane, “Quantum computing for logistics optimization: Annealing in unit load device configuration and disruption,” International Journal of Research Publication and Reviews, vol. 7, no. 6, pp. 4643–4648, 2026, doi: 10.55248/gengpi.07.0626.16a57.

[13] A. Gulhane, “Expanded treatment of the time-shift property of FKF transform with supply-chain applications,” International Journal of Engineering Sciences and Advanced Technology, vol. 25, no. 12, pp. 606–616, 2025, doi: 10.64771/ijesat.2025.v25.i12.3817.

[14] A. Gulhane, “Sequential convergence in the testing function space of the two-sided FKF transform,” International Journal of Creative and Open Research in Engineering and Management, vol. 2, no. 8, pp. 3108-1754, 2026, doi: 10.55041/ijcope.v2i8.138.

[15] A. Gulhane, “Artificial intelligence applications in sustainable logistics and green supply chain management: A bibliometric review,” International Research Journal of Modernization in Engineering Technology and Science, vol. 6, no. 12, 2024, doi: 10.56726/IRJMETS65006.

[16] J. Lee, B. Bagheri, and H.-A. Kao, “A cyber-physical systems architecture for Industry 4.0-based manufacturing systems,” Manufacturing Letters, vol. 3, pp. 18–23, 2015.

[17] F. Longo, A. Padovano, and S. Umbrello, “Value-oriented and ethical technology engineering in Industry 5.0,” Applied Sciences, vol. 10, no. 12, p. 4182, 2020.

[18] M. Christopher and H. Peck, "Building the resilient supply chain," The International Journal of Logistics Management, vol. 15, no. 2, pp. 1–14, 2004.

[19] N. Kshetri, "Blockchain's roles in meeting key supply chain management objectives," International Journal of Information Management, vol. 39, pp. 80–89, 2018.

[20] J. Preskill, "Quantum computing in the NISQ era and beyond," Quantum, vol. 2, p. 79, 2018.

[21] A. Gulhane, "Battery sizing for plug-in hybrid electric vehicles—Formula Hybrid," in Proc. 2017 IEEE International Conference on Power, Control, Signals and Instrumentation Engineering (ICPCSI), 2017, pp. 368–372, doi: 10.1109/ICPCSI.2017.8392317.

[22] A. Gulhane, A. Karale, and C. Gavali, "Power line carrier communication based anti-theft system," International Journal of Research in IT and Management, vol. 4, no. 12, pp. 1–11, 2014.

[23] A. Gulhane, A. Karale, and S. Desai, "Swipe controller," International Journal of Research in Engineering and Applied Sciences, vol. 4, no. 12, pp. 1–7, 2014.

[24] A. Gulhane, "Advancements in automotive batteries: A review," International Engineering Journal for Research & Development, vol. 8, no. 6, pp. 18–57, 2023.

[25] A. Gulhane, "Recent advances in electric vehicle battery technologies: Materials, management systems, and sustainability perspectives," International Journal of Scientific Research in Engineering and
[31] S. M. Harle, "Artificial intelligence-driven framework for village-level water conservation and groundwater sustainability," International Research
[32] V. D. Sharma, "Analyticity of Distribution Generalized Fourier-Stieltjes Transforms," 2012.

[33] V. D. Sharma, "Operators on the Distributional Generalized Two-Dimensional Fractional Fourier Transform," International Journal of Modern Mathematical Sciences, vol. 9, no. 1, pp. 39–45, 2014.

[34] V. D. Sharma and A. N. Rangari, "Operational Calculus on Generalized Fourier-Laplace Transform,"

Management, vol. 9, no. 7, pp. 1-20, 2025, doi: 10.55041/IJSREM51198.

[26] A. Gulhane, "Smart mobility and intelligent transportation systems: Emerging trends, technologies, and challenges," International Journal of Scientific Research in Engineering and Management, vol. 9, no. 11, pp. 1-10, 2025, doi: 10.55041/IJSREM53436.

[27] A. Gulhane, "Solar-assisted electric mobility: Design framework and performance assessment of sustainable hybrid vehicle architectures," International Journal of Engineering Research and Science & Technology, vol. 21, no. 3, pp. 362–368, 2025, doi: 10.56636/ijerst.2025.v21.i03.3594.

[28] A. Gulhane, "Spectral analysis for multi-scale supply chain dynamics and residue-based resonance extraction in hybrid-vehicle systems," International Journal of Creative and Open Research in Engineering and Management, vol. 2, no. 8, 2026, doi: 10.55041/ijcope.v2i8.141.

[29] A. Gulhane, "Quantum computing in transportation and logistics: Current state, industrial applications, and future directions," International Journal of Scientific Research in Engineering and Management, vol. 9, no. 9, pp. 1-10, 2025, doi: 10.55041/IJSREM52469.

[30] S. M. Harle, "Artificial intelligence for supply chain risk prediction and mitigation: A systematic review, conceptual framework, and future research agenda," International Research Journal of Modernization in Engineering Technology and Science, vol. 8, pp. 70–80, Jul. 2026.

Journal of Modernization in Engineering Technology and Science, vol. 8, pp. 31–49, Jul. 2026.

International Journal of Scientific and Innovative Mathematical Research, vol. 2, no. 11, pp. 862–867, 2014.

[35] V. D. Sharma, "Operational Calculus on Generalized Two-Dimensional Fractional Fourier Transform," International Journal of Engineering and Innovative Technology, vol. 3, no. 2, pp. 253–256, 2013.